CORRELATIONS FOR RADIATIVE NUSSELT NUMBER FOR COMBINED CONVECTION AND THERMAL RADIATION HEAT TRANSFER IN SMOKETUBE STEAM GENERATORS

Marcelo M. Galarça, mgalarca@mecanica.ufrgs.br
Francis H. R. França, frfranca@mecanica.ufrgs.br
Department of Mechanical Engineering
Federal University of Rio Grande do Sul
Porto Alegre, RS, Brazil

Abstract. *This work presents a proposition of correlations for radiative Nusselt number based on a numerical analysis of the heat transfer combining convection and thermal radiation in the turbulent flow of participating gases inside circular tubes of smoketube steam generators. Two gaseous mixtures are considered, being typical products of the combustion of methane and fuel oil. The gases temperature profiles and the heat transfer are solved by the numerical solution of the energy conservation equation. The diffusive and the convective terms are treated by the control volume method with a Flux-Spline interpolation function, while the thermal radiation is dealt with the zonal formulation. The gases radiative properties are modeled by the weighted-sum-of-gray-gases. The results include analysis of total, convective and radiative Nusselt numbers for typical conditions found in smoketube steam generators.*

Keywords: : radiative Nusselt number, heat transfer correlations, smoketube steam generators, participating gases, combined heat transfer mode

1. Introduction

The solution of the heat transfer combining convection and thermal radiation is of great importance in steam generators, furnaces for materials processing, combustors and boilers of power plants. In such processes, heat transfer from the high temperature combustion gaseous products to the system surface results from both the convective and radiative mechanisms.

Several works dealing with the combined heat transfer by convection and thermal radiation are available in the literature. Einstein (1963), Echigo et al. (1975), Smith et al. (1985), França and Goldstein (1995), Galarça and França (2006) considered the propagation of thermal radiation in both the radial and axial direction inside the tube. With the exception of the second work, which employed finite difference approximation, the other four works used a zonal-type formulation. Galarça and França (2006) presented results that include the gases bulk temperature distributions and the significance of thermal radiation in the combined heat transfer process for typical smoketube steam generators applications. Campo and Schuler (1988), and Seo et al. (1994) used the *p*-1 approximation to simplify the integral formulation of the radiation exchange to a first-order differential equation, and considered only the heat transfer in the radial direction. More recently, Sediki et al. (2002) solved the combined radiation-convection heat transfer in a circular tube employing advanced gas models, the CK-Correlated-k and the ADF-Absorption Distribution Function.

In this work, it is considered the combined heat transfer by convection and thermal radiation in the flow of combustion gases inner the circular tubes of smoketube steam generators. The analysis is based on the numerical solution of the energy conservation, where the diffusive-advective terms are treated by the Flux-Spline control volume, and the radiation terms are solved with the zonal method, considering radiation transfer in both the radial and axial directions. The dependence of the gas absorption coefficient on the wavelength is taken into account with the weighted-sum-of-gray-gases model. Two gaseous mixtures at a total pressure of 1.0 atm are considered. The first one, named gas mixture 1, is composed of water vapor (0.2 atm), carbon dioxide (0.1 atm), and nitrogen (0.7 atm), and is a typical product of stoichiometric combustion of methane. The second one, gas mixture 2, is composed of water vapor (0.1 atm), carbon dioxide (0.1 atm), and nitrogen (0.8 atm), and is a typical product of stoichiometric combustion of fuel oil. The tube walls are diffusive, gray emitters and absorbers. The gases physical properties are computed at the average bulk temperature, that is, the arithmetic mean between the gas inlet and outlet temperatures. The fluid flow is turbulent and developed in the entrance, while the temperature inlet is assumed uniform, so that the thermal entrance region is considered. The inlet and outlet reservoirs are treated as black surfaces at the temperature of the reservoirs.

Correlations are proposed for the total Nusselt number, which takes into account both radiation and convection. The correlations, applied to situations that are found in small and medium sized smoketube steam generators, are validated statistically by the comparison with the results obtained from the numerical solution.

2. Problem analysis

The problem consists, in a simplyfied form, in a tube with inner diameter and length *D* and *L*, respectively. An internal emissivity surface $\varepsilon = 0.8$ was adopted. The gas inlet temperature, T_g, and the surface temperature, T_S, are assumed as uniform. According to Galarça and França (2006) the condition of uniform temperature in the tube is a satisfactory approximation for this case. Thus, the surface temperature can be approximated by the water liquid-vapor saturation temperature at the operation pressure of the vapor line. The internal flow is turbulent and developed at the entrance, but the gas inlet temperature is assumed uniform. As it occurs in steam generators, the gas temperature is higher than the tube temperature, so that heat is transferred from the gas to the tube surface. Both the radiative and the convective mechanisms are included in the analysis. To determine the heat transfer, it is necessary to determine the gas temperature distribution, which in turn requires the solution of the energy conservation equation. In dimensionless form, this equation is given by:

$$\frac{\partial}{\partial x}\left(ut-\frac{1}{\mathrm{Re\,Pr}}\frac{\partial t}{\partial x}\right)-\frac{1}{r}\frac{\partial}{\partial r}\left[r\left(\frac{1}{\mathrm{Re\,Pr}}+\frac{1}{\mathrm{Re}}\frac{\varepsilon_H}{\nu}\right)\frac{\partial t}{\partial r}\right]=-\frac{1}{\mathrm{Re\,Pr}\,N_{CR}}q_R^* \tag{1}$$

where t is the gas dimensionless temperature, $\overline{T}/T_g$; x are r the dimensionless coordinates, X/D and R/D, respectively; N_{CR} is the conduction-radiation parameter, given by $k/\left(D\sigma T_g^3\right)$, in which T_g is the gas inlet temperature; Re and Pr are the Reynolds and Prandtl number, and ε_H is the thermal eddy diffusivity to account for the thermal turbulent transport. The thermophysical properties of the gas, such as the density ρ, the kinematic viscosity ν and the thermal conductivity k are assumed constant and evaluated at the gas average bulk temperature. In this solution, the velocity profile is assumed as developed, and is given by the equation proposed by Reichardt (1951), as presented in Kays e Crawford (1980), while the thermal eddy diffusivity ε_H is computed from the model proposed by Kays and Crawford (1980) for ducts with circular cross section.

The term q_R^* is the dimensionless net volumetric radiative heat rate, given by $q_R D/\left(\sigma T_g^4\right)$, where σ is the Stefan-Boltzman constant, equal to 5.67×10^{-8} W/m^2·K^4. In the energy equation, q_R^* corresponds to the radiative energy emitted minus the energy absorbed per unit of volume in the gas element, and is evaluated by the application of the zonal method combined to the weighted-sum-of-gray-gases (WSGG) model. The zonal method involves the division of the enclosure into surface and volume zones, in which all radiative quantities (emissive power, radiosity and irradiation) are assumed uniform. The volume and surface zones in the tube are coincident to the control volumes used for the discretization of the diffusive-advective terms. According to the zonal method and the WSGG model, the net volumetric radiative heat rate for volume zone V_γ is given by:

$$q_{R_\gamma}=\frac{1}{V_\gamma}\left[4V_\gamma\sum_{i=0}^{I}\left(C_{e,i}\left(T_\gamma\right)a_i\right)\sigma T_\gamma^4-\sum_{\gamma^*=1}^{\Gamma}\overrightarrow{g_{\gamma^*}g_\gamma}\sigma T_{\gamma^*}^4-\sum_{j=1}^{J}\overrightarrow{s_j g_\gamma}q_{o,j}\right] \tag{2}$$

On the right-hand side of the above equation, in the bracket, the first term accounts for the radiation emitted by the volume zone V_γ, while the second and the third accounts for the absorption of radiation from the other volume zones V_γ and surface zones A_j, respectively. The gas-to-gas and the surface-to-gas directed-flux areas, $\overrightarrow{g_{\gamma^*}g_\gamma}$ e $\overrightarrow{s_j g_\gamma}$, are obtained from:

$$\overrightarrow{g_{\gamma^*}g_\gamma}=\sum_{i=0}^{I}\left[C_{e,i}\left(T_{\gamma^*}\right)\left(\overline{g_{\gamma^*}g_\gamma}\right)_i\right] \tag{3}$$

$$\overrightarrow{s_j g_\gamma}=\sum_{i=0}^{I}\left[C_{e,i}\left(T_j\right)\left(\overline{s_j g_\gamma}\right)_i\right] \tag{4}$$

The coefficients $C_{e,i}$ are polynomial functions that are solely dependent on the radiation source temperatures, a_i is the absorption coefficient of each gray gas of the WSGG model. For the two gas mixtures considered in this work, the values of $C_{e,i}$ and a_i are obtained from Smith *et al.*(1982).

The gas-to-gas and the surface-to-gas direct-exchange areas, $\overline{g_{\gamma^*}g_\gamma}$ and $\overline{s_j g_\gamma}$, respectively, for each absorption coefficient a_i are given by Sika (1991). The radiosity, $q_{o,j}$, corresponds to the sum of the emission and the reflection from surface A_j, and is given by:

$$q_{o,j}=\varepsilon_j\sigma T_j^4+\left(1-\varepsilon_j\right)q_{i,j} \tag{5}$$

where $q_{i,j}$ is the irradiation on surface zone A_j and T_j is its temperature.

The radiative heat flux on surface zone A_j is:

$$q_{R,j}=\left(q_{i,j}-q_{o,j}\right) \tag{6}$$

where, according to the zonal method, the irradiation $q_{i,j}$ is computed by:

$$q_{i,j} = \frac{1}{A_j}\left(\sum_{\gamma=1}^{\Gamma}\overrightarrow{g_\gamma s_j}\sigma T_\gamma^4 + \sum_{k=1}^{K}\overrightarrow{s_k s_j} q_{o,j}\right) \tag{7}$$

The gas-to-surface and the surface-to-surface, $\left(\overrightarrow{g_\gamma s_j}\right)$ e $\left(\overrightarrow{s_k s_j}\right)$ are given by:

$$\overrightarrow{g_\gamma s_j} = \sum_{i=0}^{I} C_{e,i}\left(T_\gamma\right)\left(\overline{g_\gamma s_j}\right)_i \tag{8}$$

$$\overrightarrow{s_k s_j} = \sum_{i=0}^{I} C_{e,i}\left(T_k\right)\left(\overline{s_k s_j}\right)_i \tag{9}$$

where $\left(\overline{g_\gamma s_j}\right)$ and $\left(\overline{s_k s_j}\right)$ are the gas-to-surface and the surface-to-surface direct-exchange areas for a gray gas with absorption coefficient of a_i. An important relation for the direct-exchange areas for each gray gas a_i is given by:

$$4V_\gamma a_i = \sum_{\gamma^*=1}^{\Gamma}\left(\overline{g_\gamma g_{\gamma^*}}\right)_i + \sum_{j=1}^{J}\left(\overline{g_\gamma s_j}\right)_i \tag{10}$$

$$A_j = \sum_{\gamma^*=1}^{\Gamma}\left(\overline{s_j g_{\gamma^*}}\right)_i + \sum_{k=1}^{K}\left(\overline{s_j s_k}\right)_i \tag{11}$$

The above relation guarantees global conservation of the radiative energy in the enclosure. Since the computation of the direct-exchange areas involves the numerical calculation of integral terms, the above relations will be only approximately obeyed. For most of the pairs of zones, the error was as low as 0.1 %. Even so, for convergence of the numerical solution, it was necessary to multiply all the direct-exchange areas by a factor that forced the equality in Eqs. (10) and (11).

For the solution of the gas temperature from the energy conservation in Eq. (1) the following boundary conditions are adopted: at the tube entrance, $x = 0$, $r \geq 0$, the gas dimensionless temperature is uniform and equal to $t = 1.0$; at the tube wall, $x \geq 0$, $r = 1.0$, the gas dimensionless temperature corresponds to the tube wall dimensionless temperature, $t_s = T_s/T_g$. Taking advantage of the axis-symmetry, for $x \geq 0$, $r = 1.0$, the gas temperature gradient at is null, $\partial t/\partial r = 0$.

The global energy balance must be verified for each solution, as given by:

$$\dot{m}c_p\left(T_S - T_e\right) = \int_A q_T\, dA \tag{12}$$

where $q_T = q_R + q_C$, is the total heat flux on the tube wall, obtained by the sum for the radiative and convective heat fluxes, q_R and q_C, respectively. Since the gas enters with a temperature above the tube wall temperature, its temperature will decrease as it flows in the tube. The global energy conservation states that the decrease in the gas enthalpy is given by integration of the heat flux on the tube wall.

3. Smoketube steam generators

This type of steam generator can be divided into two types: vertical and horizontal. This work is focused on small and medium size, horizontal steam generators having a bank of tubes that are mounted on the headers. Gaseous combustion products flow in the interior of the tubes and transfer heat to the tube, where water in the outside is vaporized to form vapor. The tubes of medium and medium size steam generators have diameters ranging from 2 to 3 inches, while large size units can have diameter of 4 inches. The gases flow velocities range from 10 to 40 m/s to allow operation in the turbulent regime, where the heat transfer coefficient is more elevated (Shields, 1961). There is nowadays a large variety of sizes and configurations of steam generators to cover the different applications.

In this work, tubes having diameters ranging from 2 to 3½ inches were considered. The length of the tubes depends on the specified vapor generation capacity. The length of the tubes was kept at the value of 5.0 m for all cases presented in this work.

4. Numerical solution

The determination of the gas temperature distribution depends on the solution of Eq. (1). The coupling between the convection and radiation mechanisms adds considerable complexity to the problem. The iterative numerical procedure for this case was proposed by Galarça and França (2006), where the diffusive-advective terms of Eq. (1) are tackled with the Flux-Spline control volume (Varejão, 1979), which is based on the conventional control volume method (Patankar, 1980). The choice of the method aimed at allowing a less refined grid resolution for the diffusive-advective terms, still keeping an adequate accuracy, so that each control volume and radiative zone could be coincident. The grid mesh in the x direction was set as uniform, that is Δx constant, for it allows the reduction of the time to compute all pairs of direct-exchange areas by symmetry. In the radial direction, the grid was non-uniform to observe the steep variations on the gas temperature and velocity close to the tube wall.

In all cases, the domain in the radial direction, within the interval $0 \leq r \leq 0.5$, was divided into $M = 10$ elements, being more refined in the region close to the surface. The closest element to the tube wall was set to have the same dimension of the laminar sublayer, $\Delta r = 5y^+$, and the size of the other elements followed an exponential increase. Since different dimensional lengths were considered, different numbers of elements in the axial direction were employed, so that $\Delta x = 1.0$. That is, for $L/D = 60$, $N = 60$; for $L/D = 100$, $N = 100$; and so on. With this grid choice, the solution proved to be grid independent.

5. Results and dicussion

Results for the heat transfer are presented in terms of the convective, radiative and total Nusselt number, indicated by Nu_C, Nu_R and Nu_T, respectively. The convective Nusselt number is given by:

$$Nu_C(x) = -\frac{1}{t_m(x) - t_s} \left. \frac{\partial t(x,r)}{\partial r} \right)_{r=0,5} \tag{13}$$

where $t_m(x)$ is the gas dimensionless bulk temperature at position x; t_s is the tube wall dimensionless temperature, and is uniform in this problem. The radiative Nusselt number is given by:

$$Nu_R(x) = -\frac{1}{N_{CR}} \frac{1}{t_m(x) - t_s} \frac{q_o(x) - q_i(x)}{\sigma T_o^4} \tag{14}$$

The radiative Nusselt number $Nu_R(x)$ takes into account the radiation exchanges between the surface element with all the gas elements, with the other surface elements and with the inlet and outlet reservoirs. The total Nusselt number, Nu_T, considers both mechanisms, radiation and convection. Thus,

$$Nu_T(x) = Nu_R(x) + Nu_C(x) \tag{15}$$

For pure convective heat transfer, the total and the convective Nusselt numbers are the same.

At the tube entrance, Nu_C presents a higher value and tends to infinite for $x = 0$. The fluid flows through the tube till decrease the Nu_C to a limit value, Nu_{CD}, which means the thermal development flow. Before this, while Nu_C is changing, the region is denominated thermal entrance. The Nu_{CD} value for turbulent flows can be obtained by correlations presented in literature. The Gnielinski (1976) correlation provides good results when compared to the experimental results. The correlation is given by:

$$Nu_{CD} = \frac{(f/8)(\mathrm{Re}_D - 1000)\mathrm{Pr}}{1 + 12,7(f/8)^{1/2}(\mathrm{Pr}^{2/3} - 1)} \tag{16}$$

Equation (16) is available only for $0.5 < \mathrm{Pr} < 2000$ and $2300 < \mathrm{Re}_D < 5 \times 10^6$. The correlation is applicable either to uniform temperature or uniform heat transfer at the suface. The friction factor f can be obtained from the smooth tubes equation, given by

$$f = (0,790 \ln \mathrm{Re}_D - 1,64)^{-2} \tag{17}$$

In most engineering applications, the mean value of Nusselt, $\overline{Nu}$, which accounts the tube length is useful to calculate the coefficient average heat transfer. For large tube lengths, above 20 diameters, and turbulent flows, it is possible to estimate the average value of Nusselt number by the equation

$$\frac{\overline{Nu}}{Nu_{CD}} = 1 + \frac{C}{x/D} \tag{18}$$

where C is a constant value obtained from experimental data analysis. For fully developed velocity profiles its value is 1.4 [Kays and Crawford, 1980].

Table 1 compares both the developed Nusselt number, Nu_{CD}, found by the application of Eq.(16), and the value obtained from the present numerical solution for turbulent flow and pure convection case. The Prandtl number for this case is 0.88, which is a typical value for gases mixture from combustion products.

Table 1. Comparison between developed convective Nusselt numbers obtained from numerical solution and Gnielinski (1976) correlation. Pr = 0.88.

Re	$Nu_{CD)Num}$	$Nu_{CD)Lit}$	Deviation (%)
10000	33.04	33.27	0.81
20000	56.42	58.23	3.21
25000	67.25	69.49	3.33
30000	78.34	80.24	2.43

As shown in Tab. 1, the results given by the literature and the present numerical solution presents a good agreement, which means that the numerical solution of Eq.(1), without the radiative term, is satisfactory. This narrow range between the data will provide mean values of Nusselt number, $\overline{Nu}$, with a narrow deviation too.

When radiation is included, it is necessary to obtain an average value of radiative Nusselt number, given by the integration of Eq.(14). The effects of thermal radiation inclusion were discussed by Galarça and França (2006), and shows that for the combined heat transfer (convection-radiation) the literature correlations do not provide reliable results.

5.1 Correlations

To determine one or more correlations that could describe a specific process/phenomena, it is necessary, first, to know the involved variables. Galarça and França (2006) presents that the convective Nusselt number is not significantly affected by thermal radiation heat transfer for small diameters tubes. So, the literature correlations for pure convection can be applied for the convective term, and therefore, the effort to propose a correlation to calculate the total Nusselt number can be directed towards the thermal radiation term, through the radiative average Nusselt number.

The variables that influence the radiative Nusselt number, Nu_R, can be obtained from the dimensional analysis. For simplification, from the weighted-sum-of-gray-gases model and the zonal method, it was considered, a gray gas in a cavity with internal black surfaces. Equation (2), which considers the radiative energy rate emitted by gas volume, V_γ, can be rewrite in a non-dimension form as:

$$q_R^* = 4aD_i T_\gamma^{*4} - \sum_{\gamma^*}^{\Gamma} \overline{g_{\gamma^*} g_\gamma} \frac{D_i}{V_\gamma} T_{\gamma^*}^{*4} - \sum_{j=1}^{J} \overline{s_j g_\gamma} \frac{D_i}{V_\gamma} T_j^{*4} \tag{19}$$

where, the *optical thickness*, $\kappa = aD_i$, appears. The equations to calculate the direct-exchange areas can also be written in the dimensionless form. For gas-to-gas and surface-to-gas, the equations are given by:

$$\overline{g_{\gamma^*} g_\gamma} \frac{D_i}{V_\gamma} = \left(\frac{a^2}{\pi} \int_{V_{\gamma^*}} \int_{V_\gamma} \frac{\exp\left(-aS_{\gamma^*-\gamma}\right)}{S_{\gamma^*-\gamma}^2} dV_\gamma dV_{\gamma^*} \right) \frac{D_i}{V_\gamma} = \frac{\kappa^2}{V_\gamma D_i^3 \pi} \int_{V_{\gamma^*}} \int_{V_\gamma} \frac{\exp\left(-\kappa . s_{\gamma^*-\gamma}\right)}{s_{\gamma^*-\gamma}^2} dV_\gamma dV_{\gamma^*} \tag{20}$$

$$\overline{s_j g_\gamma} \frac{D_i}{V_\gamma} = \left(\frac{a}{\pi} \int_{V_\gamma} \int_{A_j} \frac{\exp\left(-aS_{j-\gamma}\right)\cos\beta}{S_{j-\gamma}^2} dA_j dV_\gamma \right) \frac{D_i}{V_\gamma} = \frac{\kappa^2}{V_\gamma D_i^2 \pi} \int_{V_\gamma} \int_{A_j} \frac{\exp\left(-\kappa . s_{j-\gamma}\right)\cos\beta}{s_{j-\gamma}^2} dA_j dV_\gamma \tag{21}$$

As observed, Eqs.(20) and (21) basically depends on the optical thickness, κ. The non-dimensional groups and the Nu_R defined by Eq.(14) shows the optical thickness as dominant variable in the thermal radiation heat transfer process. During the simulations, it was noted that the radiative energy rates was affected by the Reynolds numer. In such case, the following dimensionless groups can describe the process: κ, T_g/T_s and Re_D. As a matter of fact, two other groups should be included, L/D_i and $N_{CR} = k/\sigma D_i T_g^3$, and this way, raising objections to attainment of a correlation for radiative Nusselt number. The L/D_i considers the reservoirs effect, but for the usual situations found in steam generators, $L/D_i >> 1$, this term can be neglected. The radiation-conduction parameter, N_{CR}, connects the thermal radiation to convection process in the energy equation. As proposed, the convective and radiative Nusselt numbers calculations are independent, which implies that N_{CR} is not necessary. Actually, this is an approximation. To reduce the error caused by its exclusion, different temperatures, T_g and T_S, for each given ratio T_g/T_S were applied, varying the N_{CR} values and absorbing its effect in the radiative Nusselt number.

5.2 Experimental Design

The literature provides several correlations for the internal tube turbulent convective flow, which was obtained from numerical-experimental data. According to Galarça and França (2006), the thermal performance of the system is modified when the thermal radiation combined to convection process is considered. Therefore, in the heat transfer analysis inside the tubes of a smoketube steam generator, one should take into account not only the thermal convection, also the thermal radiation. In these cases, the correlations available in the literature cannot be satisfactory.

The proposed correlations consider the radiative effect for 180 numerical solutions for each gas mixture (mixture 1 and 2), that is, 360 simulations were performed. This way, it was considered a surface temperature range from 450K to 600K, which is the water vapor outside the tubes. For the inlet gas temperatures, T_g, values from 1000K to 2400K were adopted [Spring, 1940]. The diameters were chosen according to ASTM standards (ASTM A-192) and its application to steam generators; 2.77mm for thickness and diameters varying from 50.8 to 88.9mm. The tube length was fixed on 5m. The Reynolds number range depends on typical velocities values for this type of system. According to Babcock and Wilcox (1972), the range is from 15m/s to 35m/s. However, if the simulations take into account only these velocity limits, just a few data would be obtained. So, for application of a regression model it was necessary a larger range. The velocity values applied were between 10m/s and 100m/s. This kind of extrapolation was useful to guarantee a good sample of results for the correlations proposal.

To generalize the problem, four ratios were adopted, T_g/T_s = 2, 3, 4 and 5. For each ratio, three different values for T_g and T_s were adopted, ensuring that these values does not influence the process, keeping the main ratio. The diameters values affect directly the optical thickness, $\kappa = a_{médio} D_i$. For this case, a mean absorption coefficient was used for each gas mixture, $a_1 = 1,411\text{m}^{-1}$ and $a_2 = 1,9548\text{m}^{-1}$, for mixture 1 and 2 respectively. As result, 180 radiative average Nusselt numbers, $\overline{Nu_R}$, for each gas mixture was generated from the numerical solution and, after, used for comparison with results obtained by proposed correlations in this paper.

5.2.2 Statistical Index

The statistical treatment to obtain the correlations was carried out by the application of curve fitting, leading to correlations in better agreement with the expected performance presented by the heat transfer process.

The comparison between the data generated by numerical solution and the results obtained by the proposed correlations was done using statistical parameters developed by Hanna (1989). This analysis was applied in this paper in order to validate the correlations equations obtained from the computational solution.

The subscripts "*o*" and "*p*" are used to indicate the observed (by the numerical solution) and the predicted values (by the proposed correlations) respectively; $\overline{Nu_R}$ is the radiative average Nusselt number and σ is the standard deviation. The statistical parameters applied are defined next:

Correlation Coefficient: represent the existence of a relationship between the observed data. The more correlation there is, the closer to 1 is the value, or else, "0" for no correlation and "1" for perfect correlation:

$$r = \frac{\overline{\left(\overline{Nu_{R,o}} - \overline{\overline{Nu_{R,o}}}\right)\left(\overline{Nu_{R,p}} - \overline{\overline{Nu_{R,p}}}\right)}}{\sigma_o \sigma_p} \quad (22)$$

Normalized Mean Squared Error: this value indicates all deviation between the predictions and the observed values. That is a non-dimensional statistical value. Its result should be the smaller as possible to represent an accurate model:

$$Nmse = \frac{\overline{\left(\overline{Nu_{R,o}} - \overline{Nu_{R,p}}\right)^2}}{\overline{\overline{Nu_{R,o}} \times \overline{Nu_{R,p}}}} \quad (23)$$

Factor Two (Fa2): it is the fraction of the predictions that are within a factor two of the measurements:

$$0.5 \le \overline{Nu_{R,p}} \big/ \overline{Nu_{R,o}} \le 2 \quad (24)$$

Fractional Bias (Fb): it is a number that represent the model tendency to over or underestimate the observed values. The best result is zero:

$$Fb = \frac{\overline{\overline{Nu_{R,o}}} - \overline{\overline{Nu_{R,p}}}}{0.5\left(\overline{\overline{Nu_{R,o}}} + \overline{\overline{Nu_{R,p}}}\right)} \quad (25)$$

Fractional Standard Deviation (Fs): it makes a link between the observed and predicted values, that is, it indicated how far the data from the "actual" value is. The optimum result is zero:

$$Fs = 2\frac{\sigma_o - \sigma_p}{\sigma_o + \sigma_p} \tag{26}$$

5.2.3 Correlations

With the 180 radiative average Nusselt numbers, $\overline{Nu_R}$, for each gas mixture, obtained from the numerical solution, the analysis can be carried out applying an average operation over the $\overline{Nu_R}$ values. To group sample data developing analysis of its behavior on the basis of the average values is a form to increase the final result probability to present good trustworthiness [Montgomery, 1997].

In accordance with the experimental design, it had been considered for each temperature ratio, $T^*=T_g/T_s$, three different values for T_g and T_s; as result, for each optical thickness value, κ , fifteen different values of $\overline{Nu_R}$ were gotten. Thus, for each κ , after calculating the averages of all $\overline{Nu_R}$ values, five results (one for each Re_D value) were taken for the problem analysis. Therefore, each one of the gas mixtures has its behavior observed with the $\overline{Nu_R}$ variation in relation to T^*, for the Re_D range from 10000 to 30000. This is shown in Fig. 1a and 1b.

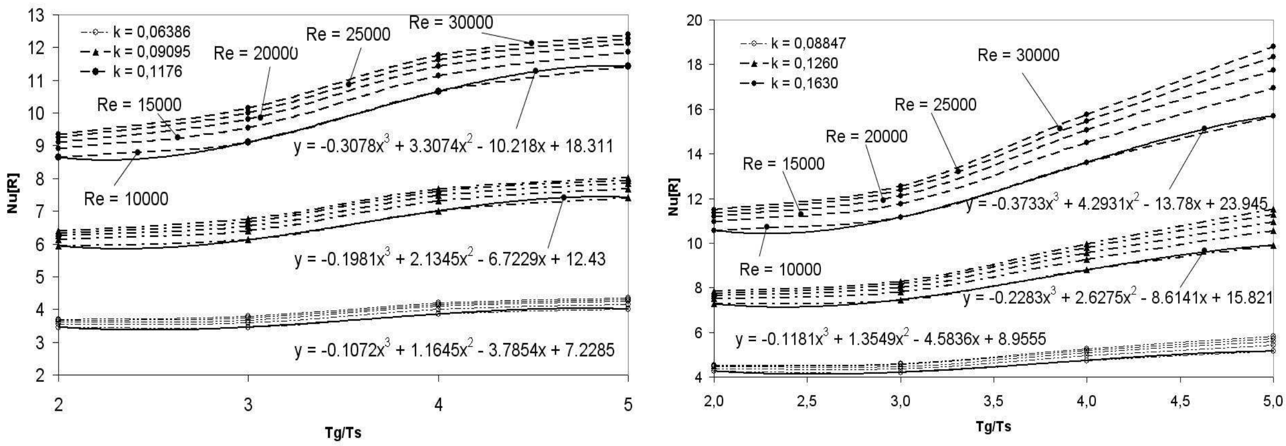

(a) (b)

Figure 1 Variation of $\overline{Nu_R}$ with T_g/T_S and curve fitting for the Mixtures 1 (a) and 2 (b).

Figure 1 present the dependence of the radiative average Nusselt number on the temperature ratio, T_g/T_s, for different optical thickness and Reynolds number values. It was presented the curve fitting to illustrate the relation between $\overline{Nu_R}$ and T_g/T_s for Re_D = 10000. As can be observed, a third order polynomial curve shows a good agreement to describe the phenomenon. Besides, it can be observed that, for both cases (mixtures 1 and 2) the $\overline{Nu_R}$ is significantly influenced by optical thickness, κ , which depends on the inner diameter. This reinforces the results presented by Galarça and França (2006). However, the Reynolds number influence is not as significant as T_g/T_S and κ but will be taken into account too.

Once it was obtained the curve fittings for both cases in which Re_D = 10000 for each aspect ratio, L/D_i, it is necessary to know how to correlate the optical thickness, κ , with the radiative average Nusselt numbers. This was accomplished from the coefficients (*A*, *B*, *C* and *D*) behavior analysis for each cubical equation. In a general form, the equation can be presented as:

$$\overline{Nu_R} = -A\left(\frac{T_g}{T_S}\right)^3 + B\left(\frac{T_g}{T_S}\right)^2 - C\left(\frac{T_g}{T_S}\right) + D \tag{27}$$

The coefficients values are shown in the Figs.2(a) and 2(b) for mixtures 1 and 2, respectively.

As can it be observed, the curve fitting was done using different optical thickness values, $\kappa = aD_i$, due to its considerable influence on the radiation heat transfer process, according to earlier discussions. The optical thickness values are limited only by the aspect ratio, L/D_i, because it is a diameter dependent variable. Therefore, the applicable range of the proposed correlations is $60 \le L/D_i \le 110.5$, which is appropriate to steam generation systems considered in this work.

The equations for the coefficients, generated by the curve fitting, are inserted into the Eq.(27) for each gas mixture. It can be observed from the Tab. 2, which shows how to use the equation model.

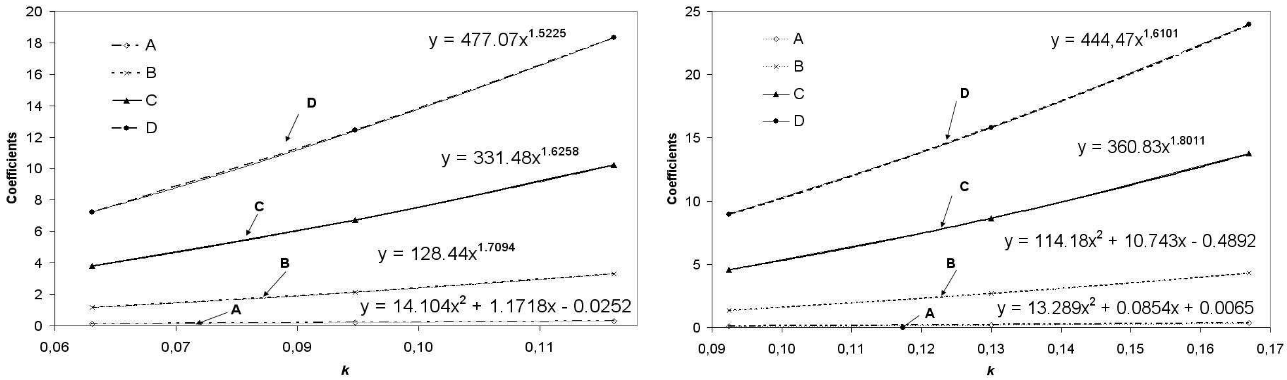

(a) (b)

Figure 2 Curve fitting: coefficients analysis (Eq. (27)) for Gaseous Mixtures 1(a) and 2 (b).

Table 2 Coefficients for application into Eq. (27). Gas Mixtures 1 and 2.

$$\overline{Nu_R}\Big)_{Re_D=10000} = -A\left(\frac{T_g}{T_s}\right)^3 + B\left(\frac{T_g}{T_s}\right)^2 - C\left(\frac{T_g}{T_s}\right) + D$$

Coefficient	Mixture 1	Mixture 2
A	$14.104(\kappa)^2 + 1.1718(\kappa) - 0.0252$	$13.289(\kappa)^2 + 0.0854(\kappa) + 0.0065$
B	$128.44(\kappa)^{1.7094}$	$114.18(\kappa)^2 + 10.743(\kappa) - 0.4892$
C	$331.48(\kappa)^{1.6258}$	$360.83(\kappa)^{1.8011}$
D	$477.07(\kappa)^{1.5225}$	$444.47(\kappa)^{1.6101}$

The results obtained from Eq.(27) by using the coefficients presented in Tab. 2 were generated for $\overline{Nu_R}\Big)_{Re_D=10.000}$. In other words, for the radiative average Nusselt numbers when $Re_D = 10000$, due to the cubical curve showed in the Fig.1. This way, from the described curves it is possible to establish a $\overline{Nu_R}$ dependence with the Reynolds number variation based on the $\overline{Nu_R}\Big)_{Re_D=10.000}$ values. So,

$$\overline{Nu_R} = \overline{Nu_R}\Big)_{Re_D=10.000}\left(\frac{Re_D}{10.000}\right)^n \tag{28}$$

The exponent n was obtained from computational solution results for Reynolds numbers 10000, 15000, 25000 and 30000, using the $\overline{Nu_R}$ and $\overline{Nu_R}\Big)_{Re_D=10.000}$ data, for each L/D_i and T_g/T_S.. After statistical analysis, the values with a better agreement to computational solution were chosen. This way, the application of Eq. (28) can be made with n values, as follow:

$$\begin{aligned} n &= 0.09778 \quad \text{(Mixture 1)} \\ n &= 0.07934 \quad \text{(Mixture 2)} \end{aligned} \tag{29}$$

5.2.4 Application of correlations

Now, the practical validation of the correlations is made determining values for $\overline{Nu_R}$ based on the numerical solution. Tables 3 and 4 show the comparison between $\overline{Nu_R}$ results for both gaseous mixtures generated by numerical solution and the application of the correlation.

Table 3 – Comparison between computational solution and correlation results for $\overline{Nu_R}$. Mixture 1.

T_g/T_s	κ	Re_D	$\overline{Nu_R}$ (Comp. Solution)	$\overline{Nu_R}$ (Correlation)	Deviation(%)
2.5	0.06386	10000	3.345	3.383	1.164
3.5	0.06386	14380	3.937	3.802	3.413
4.5	0.09095	19547	7.345	7.765	5.712
5	0.11762	30040	12.344	12.846	4.070

Table 4 – Comparison between computational solution and correlation results for $\overline{Nu_R}$ **.** Mixture 2.

T_g/T_s	κ	Re_D	$\overline{Nu_R}$ (Comp. Solution)	$\overline{Nu_R}$ (Correlation)	Deviation(%)
2.5	0.08847	10000	4.102	4.142	0.980
2.5	0.08847	31596	4.450	4.635	4.149
3.5	0.16295	20502	14.151	13.327	5.824
4.5	0.12601	18941	9.492	9.802	3.266

Although a low deviation for the above results can be observed, this behavior was not observed for all the entire data of the 180 simulations for each gas mixture. In some few cases, deviations around 17% and 15% for mixture 1 and 2, respectively, were observed, it occurs due to the low optical thickness values, in other words, for diameters below $2\frac{1}{4}''$ (57.15mm). However, these cases are dominated by convection heat transfer, and this way the thermal radiation error has just a small effect on the final result. The statistical indexes described in section 5.2.2 were used for validation of the results, which is presented in Table 5.

Table 5 – Statistical Index for the two gaseous mixtures.

Gas Mixture 1				
Nmse	*R*	*Fa2*	*Fb*	*Fs*
0,001	0,988	1,000	-0,009	-0,001
Gas Mixture 2				
Nmse	*R*	*Fa2*	*Fb*	*Fs*
0,010	0,984	1,000	-0,002	0,058

As can be observed in the Table 5, the correlation results have a good agreement with the computational results. The correlation coefficient, *R*, is closer to the optimum value, which is 1 (one), for both gaseous mixtures. These results are reinforced by the others statistical indexes. The *Nmse* for mixtures 1 and 2, were also low. According to Hanna (1989), this value should be as small as possible in order to guarantee a good model. The *Fa2* shows that 100% of obtained results are in agreement to the limit range which is confirmed by the others statistical indexes, *Fb* and *Fs*. Therefore, the validation determines that the $\overline{Nu_R}$ values are appropriate for conditions considered in this work.

Finally, the correlations can be used to find the total average Nusselt number, $\overline{Nu_T}$, by averaging Eq.(15). According to Galarça and França (2006), the convective and radiative average Nusselt numbers can be obtained in a separate form.

Table 6 – Comparison between the computational solution and proposed correlation results for $\overline{Nu_T}$.

T_g/T_s	κ	Re_D	$\overline{Nu_T}$ (Comp. Solution)	$\overline{Nu_T}$ (Correlation)	Desviation (%)
Gas Mixture 1					
2.5	0.11762	16734	58.90	59.32	0.71
3.5	0.09095	14454	47.56	51.10	7.44
4.5	0.14110	21585	74.89	79.56	6.24
5	0.11762	10000	43.57	44.42	1.95
Gas Mixture 2					
2	0.12601	10000	39.67	40.31	1.61
3	0.12601	25000	73.11	78.15	6.89
3.5	0.16295	20500	71.52	74.92	4.75
5	0.16295	15000	63.84	66.14	3.60

The first one can be obtained by available correlations in the literature and the second one, by using the proposed correlations in this work. Table 6 presents the comparative results between $\overline{Nu_T}$ generated by the computational solution and those obtained from the proposed correlations. The proposed correlations can be applied in the following ranges:

$$10000 \le \mathrm{Re}_D \le 30000;\ 60 \le L/D_i \le 110{,}5;\ 2 \le T_g/T_s \le 5 \ \text{ for }\ 450\mathrm{K} \le T_s \le 600\mathrm{K}$$
$$0.06 \le \kappa \le 0.124 \text{ for Mixture 1; } 0.08 \le \kappa \le 0.163 \text{ for Mixture 2} \quad (30)$$

6. Conclusions

This paper presented correlations for the radiative average Nusselt number obtained from a statistical analysis of the numerical solution for combined radiation and convection heat transfer process. Turbulent flow of partipating gases inside circular tubes was considered, according to the conditions found in smoketube steam generators. In this case, the wall temperature can be assumed uniform and equal to the vapor saturation temperature at a given operational pressure. The diffusive-advective and the radiative terms of the energy equation were treated by the Flux-Spline control volume and by the zonal methods, respectively (Galarça and França, 2006). Two gaseous mixtures were considered, being typical products of the combustion of methane and fuel oil. Their radiative properties were modeled by the weighted-sum-of-gray-gases.

The correlations were proposed for the total Nusselt number, which takes into account both radiation and convection. This step requires initially a dimensional analysis to reduce the number of independent parameters. The correlations, applied to situations that are found in small and medium sized smoketube steam generators, are validated statistically by the comparison with the results obtained from the numerical solution.

7. Acknowledgments

The authors thank CNPq (Brazil) for the support under a Doctor Degree scholarship.

8. References

ASTM A192 / ASME SA192, Seamless Carbon Steel Boiler Tubes for High Pressure Service.

Echigo, R.. et al., 1975, "Composite Heat Transfer in a Pipe with Thermal Radiation of Two-Dimensional Propagation - in Connection with the Temperature Rise in Flowing Medium Upstream from Heating Section", Int. J. Heat Mass Transfer, Vol. 18, pp. 1149-1159.

Einstein, T.H., 1963, "Radiant Heat Transfer to Absorbing Gases Enclosed in a Circular Pipe with Conduction, Gas Flow, and Internal Heat Generation", NASA TR R-156, 28 pp.

França, F. H. R., e Goldstein Jr., L., 1998, "Effects of Temperature and Geometry on the Heat Transfer from Turbulent Flow of a Participating Gas Through a Duct", Heat Transfer Engineering, Vol. 19, pp. 25-33.

Galarça, M. M., França, F. H. R., 2006, "Effect of Thermal Radiation In The Heat Transfer In Smoketube Generators", ENCIT2006 – 11th Brazilian Congress of Thermal Sciences and Engineering, Curitiba, Brazil, Dec.5-8.

Kays, W. M., e Crawford, M. E., 1980, "Convective Heat and Mass Transfer", McGraw Hill Book Company, 2nd edition.

Montgomery, D. C., 1997, "Design and Analysis of Experiments", 4th Edition, John Wiley & Sons, New York.

Patankar, S. V., 1980, "Numerical Heat Transfer and Fluid Flow", Hemisphere Publishing Corporation.

Reichardt, H., 1951, Arch. Ges. Warmetechnik, Vol. 6/7, cited in Kays e Crawford (1980).

Schuler, C, e Campo, A., 1988, "Numerical Prediction of Turbulent Heat Transfer in Gas Pipe Flows Subject to Combined Convection and Radiation", Int. J. Heat and Fluid Flow, Vol. 9, No. 3, pp. 308-315.

Sediki, E., Soufiani A., Sifaoui, M. S., 2002, "Spectrally Correlated Radiation and Laminar Forced Convection in the Entrance Region of a Circular Duct", Int. J. Heat and Mass Transfer, Vol. 45, pp. 5069-5081.

Seo, T., Kaminski, e Jensen, M. K., 1994, Combined Convection and Radiation in Simultaneously Developing Flow and Heat Transfer with Nongray Gas Mixtures", Numerical Heat Transfer, Part A, Vol. 26, pp. 49-66.

Shields, C. D., 1961, "Boiler: Types, Charateristics and Functions", F. W. Dodge Co. New York.

Sika, J., 1991, "Evaluation of Direct-Exchange Areas for a Cylindrical Enclosure", ASME J. of Heat Transfer, Vol. 113, pp.1040-1044.

Smith, T. F., Shen, Z. F., e Friedman, J. N., 1982, "Evaluation of Coefficients for the Weighted Sum of Gray Gases Model", ASME Journal of Heat Transfer, Vol. 104, pp. 602-608.

Smith, T. F., et al., 1985, "Radiative and Convective Transfer in a Cylindrical Enclosure for a Real Gas", ASME Journal of Heat Transfer, Vol. 107, pp. 482-485.

The Babcock & Wilcox Company, 1972, "Steam: Its Generation and Use". 38th edition. New York.

Varejão, L. M. C., 1979, "Flux-Spline Method for Heat, Mass, and Momentum Transfer". Minnesota: Faculty of the Graduate School of the University of Minnesota, 235 p. Thesis.

9. Copyright notice